

## A Technique for Generating Idealized Initial and Boundary Conditions for the PSU–NCAR Model MM5

HUI-YA CHUANG AND PETER J. SOUSOUNIS

*Atmospheric, Oceanic, and Space Sciences Department, The University of Michigan, Ann Arbor, Michigan*

(Manuscript received 13 October 1998, in final form 11 November 1999)

### ABSTRACT

A new idealized initialization technique has been developed for the Mesoscale Model version 5 modeling system. The technique allows the specification of baroclinic disturbances that feature vertical variations of the height, temperature, and wind fields in terms of phase lag, wavelength, and phase speed. The technique involves specifying a sounding profile at some reference point, generating the desired height fields using an analytic formulation, constructing the wind fields to be in geostrophic balance, and generating temperature fields using the hydrostatic relationship.

A distinct advantage of this technique over existing ones is that the boundary conditions are not restricted to being specified as periodic. The flexibility means that 1) users do not have to specify a domain whose size is equal to an integer number of wavelengths of the specified flow; 2) users can specify a flow that consists of different wavelengths at different heights, as is typically observed; and 3) any responses that are generated orographically or thermally in the domain and which leave the eastern boundary will not reenter the western boundary. This last item is particularly advantageous because it allows users to study the effects of a preconditioned environment on subsequent development of a featured disturbance rather than studying the repetitive effects of the same forcing mechanism on the same disturbance.

Examples of simulations using initial conditions that are generated with this technique are shown for 1) zonal flow and 2) continuous sinusoidal waves. Flat terrain was adopted for both examples. In example 1, the boundary layer parameterization scheme and surface fluxes were turned off for a simplified zonal flow situation to demonstrate the stability of this technique. During the simulations, the flow remained zonal, exactly as specified, even after 48 h. In example 2, a situation consisting of continuous sinusoidal waves moving across an array of four warm circular lakes was created to demonstrate the utility of the technique for examining how disturbances may be affected by the Great Lakes. Realistic-looking highs, lows, and fronts, along with individual and lake-aggregate enhancements developed by 48 h. Good stability and lack of distortion throughout the domain in both examples add credibility to the technique.

### 1. Introduction

The Pennsylvania State University–National Center for Atmospheric Research (NCAR) Mesoscale Model version 5 (MM5) has been available to the meteorological research community since the early 1990s (Dudhia 1993). An NCAR-supported workstation version has been available since the mid-1990s. This availability has allowed researchers the flexibility of performing simulations locally and, perhaps, more cheaply if not more quickly than could otherwise be done using remotely accessible supercomputers. For example, Ballentine et al. (1998) used MM5 to forecast lake-effect storms over Lake Ontario in real time on a workstation and found good agreement between model simulations and obser-

vations. Additionally, MM5 is configured so that sensitivity simulations can be performed to examine the effects of surface fluxes, convection, latent heating, etc., simply by changing the values of appropriate switches within easy-to-reach areas of the model code. The widespread availability of MM5, its flexibility to run on different platforms, its user-friendly format, and the fact that it is strongly supported by NCAR have made MM5 a popular choice among modelers.

The availability to use MM5 for performing various sensitivity simulations to study the effects of various physical processes in real case studies has existed for some time. However, the capability to use MM5 to examine the effects of various aspects of the flow, of different types of flows, or of synoptic-scale features on development has effectively been lacking. Other modeling systems have enjoyed limited utility from various routines that generate idealized initial conditions (ICs) and boundary conditions (BCs). For example, Sun and Chern (1994) used uniform zonal flow as initial conditions for the Purdue Mesoscale Model to simulate flow

---

*Corresponding author address:* Dr. Peter J. Sousounis, Atmospheric, Oceanic, and Space Sciences Department, The University of Michigan, Ann Arbor, MI 48109-2143.  
E-mail: sousou@umich.edu

past idealized mountains. Cao and Cho (1995), as well as Chen and Frank (1993), described a technique for generating idealized initial and boundary conditions regarding synoptic-scale features in MM4, which was the predecessor to MM5. The technique was based on an analytic formulation by Fritsch et al. (1980) and Nuss and Anthes (1987). Stauffer et al. (1993) developed a generalized initialization technique that was used for preliminary testing of the nonhydrostatic capabilities of MM5 in three dimensions and was especially useful for complex terrain (mountain–valley, land–sea-breeze studies). The code assumes that the initial wind field does not vary on a pressure surface, and that the mass fields vary on a pressure surface based on the specified wind and mass profile at some location and the wind shear. The sea level pressure field is based on geostrophy and the virtual temperature gradients on a pressure surface depend on the specified wind shear through thermal wind balance. Colle and Mass (1998) used a version of this technique with MM5 to examine various responses to idealized zonal flows over mountains.

The above-mentioned techniques have limitations of one sort or another. For example, the technique developed by Stauffer et al. (1993) and used by Colle and Mass (1998) is too restrictive in that it allows vertical but not horizontal variations and so does not allow specification of preexisting disturbances. Although the technique developed by Fritsch et al. (1980) could be easily adapted to the MM5 modeling system, some features make it unsuitable for our purposes. First, the fact that the temperature field needs to be specified analytically to determine the height field hydrostatically makes it difficult to specify conditions such that surface lows, for example, lag 500-hPa troughs by a specified amount at a specified time. Second, the use of periodic east–west boundary conditions, which requires the domain size to be an integer multiple of the wavelength, makes it difficult to specify different wavelengths for different vertical levels as is typically observed. Third, when simulating disturbances that are generated by geographic features within the domain (e.g., an aggregate of lakes in our case), it is undesirable to have the disturbances that have been developed by these features reenter the domain.<sup>1</sup> Finally, the channel model assumption prevents flow from crossing the north and south boundaries.

The purpose of this paper is to document a newly developed procedure for generating idealized ICs and BCs for MM5 to study more complicated scenarios. The procedure is based on the one developed by Stauffer et al. (1993). Although it has not yet been tested over complex terrain, it allows the user much greater flexibility in terms of specifying initial conditions that are more complicated than those specified from a single sounding, for

example. The technique itself is described in detail in section 2. Two examples of different types of ICs are provided in section 3. Actual MM5 simulations using the idealized ICs and BCs from both examples are also presented to demonstrate the validity of the procedure. Closing remarks are presented in section 4.

## 2. Idealized initialization technique

The MM5 modeling system contains four preprocessing routines that generate the static initial and boundary conditions: TERRAIN, DATAGRID, RAWINS, and GRIN. The routine TERRAIN is used to specify terrain height, land use, and model domain characteristics. The routine DATAGRID is then used to obtain data at each grid point within the domains from the NCAR data archives for the desired period of time. Because the resolution of the NCAR data archives is rather coarse, the grid can be refined by incorporating rawinsonde and standard network data using a successive scan Cressman technique in RAWINS. The routine GRIN is used as the final preprocessing step to perform vertical interpolation from pressure to sigma levels. Before the interpolation is done, GRIN is used to recalculate sea level pressure and to compute vertical velocity. In addition, ICs from DATAGRID or RAWINS are used by GRIN to generate the BCs that are needed as input for MM5 at a user-specified frequency after the initial time.

In the idealized technique, the idealized terrain height, land use, and model domain characteristics are specified within TERRAIN. The surface pressure, relative humidity, height, wind, and temperature fields are then specified on global latitude–longitude grids within DATAGRID before interpolation to model grids is performed. The purpose for specifying fields on global grids instead of model grids is so that this method is independent of map projection choice. The stepwise procedure may be summarized as follows:

- step 1—specify the temperature and humidity profiles at a chosen grid point,
- step 2—generate the height fields using an analytic formulation,
- step 3—determine the velocity fields using the geostrophic relationship,
- step 4—specify the relative humidity fields,
- step 5—construct the virtual temperature fields, and
- step 6—generate the surface pressure field.

These steps are described in detail below.

*Step 1:* Specify the temperature and humidity profiles along with the sea level pressure at a chosen grid point (point A in Fig. 1), for example, based on the typical sounding profile of a cold air outbreak. The virtual temperature  $T_v$  is calculated at each level using the formulation

$$T_v(x_a, y_a, p, t = 0) = T(x_a, y_a, p, t = 0)(1 + 0.608W), \quad (2.1)$$

<sup>1</sup> The periodic boundary conditions mean that the perturbations that leave the eastern boundary reenter the western boundary.

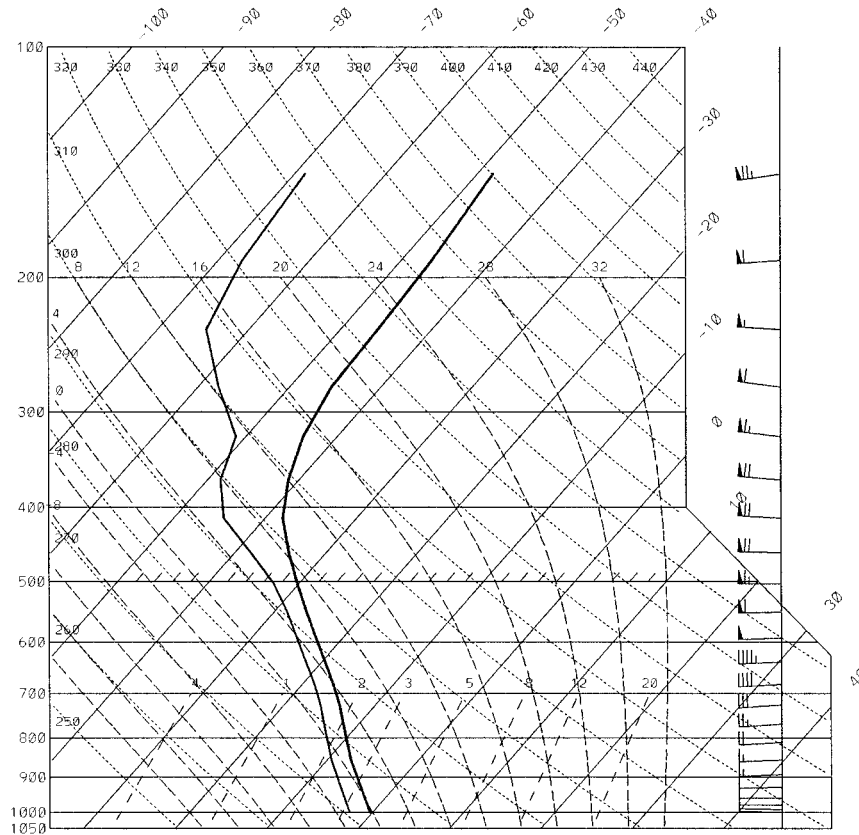


FIG. 1. Initial sounding for examples 1 and 2 at point A (45, 87).

where  $(x_a, y_a)$  are the  $(x, y)$  coordinates of point A and  $W$  is the specific humidity. The horizontal coordinates  $(x, y)$  are given as distance in meters from the origin in the zonal and meridional directions respectively. The origin is set to be at  $(0^\circ\text{N}, 0^\circ\text{E})$  in our case. The height at the chosen grid point  $H_A(p)$  must then be calculated at each mandatory pressure level  $p$  (e.g., 1000, 850, 700, 500, 400, 300, 250, 200, 150, 100 hPa) using the hydrostatic relationship:

$$H_A(p) = H_A(p + \Delta p) - R \frac{\bar{T}_v}{g} \ln\left(\frac{p}{p + \Delta p}\right), \quad (2.2)$$

where

$$R = \text{universal gas constant and}$$

$$\bar{T}_v = [T_v(x_a, y_a, p, t = 0) + T_v(x_a, y_a, p + \Delta p, t = 0)]/2.$$

Step 2: Generate the height fields using an analytic formulation, for example,

$$H(x, y, p, t) = H_A(p) - a(p)(y - y_a) + h(x, y, p, t) - h(x_a, y_a, p, t = 0), \quad (2.3)$$

where

$$h(x, y, p, t) = h' \left[ C_1 + C_2 \frac{\ln(1000/p)}{\ln(1000/p_0)} \right] \exp\left[-\frac{(y - y_0)^2}{b_y^2}\right] \times \sin\left\{\frac{2\pi}{L_x(p)}[x - x_0(p) - c(p)t]\right\},$$

$$a(p) \cong u_g(p)f/g,$$

$$u_g(p) = u_{1000} + \text{dudp} \times (1000 - p)/100,$$

$$L_x(p) = L_{x1000} + (L_{x500} - L_{x1000}) \frac{\ln(1000/p)}{\ln(1000/500)},$$

$$x_0(p) = x_{01000} - [\text{tilt} \times \text{dcdp} \times 5 + \text{ltilt}(p)]$$

$$\times \frac{\ln(1000/p)}{\ln(1000/500)},$$

$$c(p) = c_{1000} + \text{dcdp} \times (1000 - p)/100, \quad \text{and}$$

$$\text{ltilt}(p) = L_x(p)/4.$$

The verbal definitions for some of the variables in (2.3) are

- $f$  = Coriolis parameter ( $\text{s}^{-1}$ ),
- $g$  = acceleration due to gravity ( $\text{m s}^{-2}$ ),
- $u_{1000}$  = zonal wind speed at 1000 hPa ( $\text{m s}^{-1}$ ),

- $dudp$  = upward change in zonal wind speed [ $m\ s^{-1}$  ( $100\ hPa$ ) $^{-1}$ ],  
 $h'$  = amplitude of the wave (m),  
 $b_y$  = wave amplitude decay scale in meridional direction (m),  
 $C_1, C_2$  = constants related to variation of wave amplitude with pressure,  
 $x_0(p), y_0$  = location of trough center in zonal and meridional directions at initial time (m),  
 $x_{01000}$  =  $x$  location of trough at 1000 hPa at initial time (m),  
 $ttilt$  = simulation time when optimal tilt is desired to occur (s),  
 $dcdp$  = upward change in zonal phase speed [ $m\ s^{-1}$  ( $100\ hPa$ ) $^{-1}$ ],  
 $p_0$  = pressure level for maximum wave amplitude (hPa),  
 $L_x(p)$  = wavelength of the disturbance (m),  
 $L_{x1000}$  = wavelength at 1000 hPa (m),  
 $L_{x500}$  = wavelength at 500 hPa (m),  
 $c(p)$  = zonal phase speed of the disturbance ( $m\ s^{-1}$ ), and  
 $c_{1000}$  = zonal phase speed at 1000 hPa ( $m\ s^{-1}$ ).

This particular formulation [Eq. (2.3)] generates a pattern of continuous sinusoidal waves with wavelength  $L_x$ , wave amplitude  $h'$ , and zonal phase speed  $c(p)$ . The correct specification of  $c(p)$  is very important when there are disturbances in the initial conditions (e.g., when  $h'$  is specified to be nonzero) even though it will not affect the simulated phase speed (e.g., the speed at which the disturbance actually moves in the simulation). As mentioned previously, the boundary conditions are updated at a user-specified frequency in MM5. Therefore, contamination at the boundaries is likely to occur when the simulated phase speed of the disturbance is not equal to the user-specified value of  $c(p)$ . Thus, it is recommended that the user defines  $c(p)$  to be the same at all levels based on the Rossby wave phase speed formulation (Haltiner and Williams 1980) at some steering level (e.g., 700 hPa) initially:

$$c(p) = u_g(p_{steer}) - \frac{\beta L_x^2(p_{steer})}{4\pi^2},$$

$$p = \text{all levels}, \quad (2.4)$$

where  $p_{steer}$  is the pressure at the steering level and  $\beta$  is the meridional gradient of  $f$ . The user should then ideally perform a preliminary simulation over an extended coarse grid, and should ultimately refine the values of  $c(p)$  at each level by substituting the initially specified values with the phase speeds exhibited in the simulation. The initial specification of a constant  $c(p)$  at all levels will typically lead to an overestimated phase speed near the surface and an underestimated phase speed at upper levels. Although case dependent, the corresponding adjustment for typical synoptic-scale systems at midlatitudes will be on the order of a few meters per second below 500 hPa.

If the disturbance of interest (e.g., featured disturbance) is not specified to enter the domain until later in the simulation, then one of the following two methods needs to be used to ensure that it as well as all other upwind waves are properly captured as they enter the model domain. The first method is to choose a correct boundary condition period ( $T$ ) based on  $c(p)$  and  $L_x(p)$ :

$$T \leq \frac{L_x(p)}{4c(p)}. \quad (2.5)$$

The second method is to use a coarse grid mesh domain, which surrounds the original domain, and which already includes the featured upwind disturbance. This method has the added advantage of reducing contamination at the boundaries of the fine mesh domain because, regardless of how well the lateral boundary conditions can be prespecified for unforced flow, the presence of any kind of thermal or mechanical forcing as part of a simulation will disturb the flow and create the possibility of strong gradients to develop at the downwind boundaries. A sufficiently large and appropriately situated coarse mesh domain with a sponge boundary will help prevent not only the artificially strong gradients from developing in the first place but will also help prevent contamination in the fine grid mesh, which is the domain of interest.

The values of  $a(p)$  in (2.3) are given based on the desired wind speed  $u_g(p)$  at each pressure level. The vertical variation of  $u_g(p)$  should be chosen according to the desired meridional temperature gradient. Note that in (2.3), because the zonal wind speed is desired to vary mainly in the vertical direction for simplicity,  $a(p)$  is merely a function of pressure. The variation of  $x_0(p)$  in the vertical direction is specified in a way so that the optimal tilt (one-quarter wavelength) of the featured trough between 1000 and 500 hPa occurs at the desired time  $ttilt$ . By optimal tilt, it is meant here that the 500-hPa featured trough lags the 1000-hPa featured low by one-quarter wavelength.

*Step 3:* Determine the velocity fields using the geostrophic relationship,

$$u(x, y, p, t) = -\frac{g}{f} \frac{\partial}{\partial y} H(x, y, p, t) \quad \text{and}$$

$$v(x, y, p, t) = +\frac{g}{f} \frac{\partial}{\partial x} H(x, y, p, t). \quad (2.6)$$

If this geostrophic constraint yields winds that are undesirably different from those based on gradient wind balance, then a substitution can easily be made.

*Step 4:* Specify the relative humidity fields. The current formulation of this technique limits specification to constant values on pressure surfaces.

*Step 5:* Construct the virtual temperature fields from the ground up using the hydrostatic relationship,

$$\bar{T}_v(x, y, p, t) = -\frac{g[H(x, y, p + \Delta p, t) - H(x, y, p, t)]}{R \ln\left(\frac{p}{p + \Delta p}\right)} \tag{2.7}$$

The temperature fields are then computed from the virtual temperature and relative humidity fields using an iteration method. The surface temperature  $T_{\text{sfc}}$  is specified from the interpolation or the extrapolation of the temperature fields at the two lowest mandatory levels by assuming that temperature changes linearly with height.

*Step 6:* Generate the surface pressure field using the hydrostatic relationship and the 1000-hPa height field,

$$p_{\text{sfc}}(x, y, t) = p_{\text{mand}} \exp\left\{ [H(x, y, P_{\text{mand}}, t) - Z_0(x, y)] \frac{g}{RT_{\text{mean}}} \right\}, \tag{2.8}$$

where  $P_{\text{mand}}$  is the mandatory pressure level that is closest to the surface,  $Z_0(x, y)$  is the terrain height, and

$$T_{\text{mean}}(x, y, t) = \frac{1}{2} [T(x, y, P_{\text{mand}}, t) + T_{\text{sfc}}(x, y, t)]. \tag{2.9}$$

The last step in the idealized initialization process is to modify the idealized ground temperature (including water temperatures) in GRIN. For land points, the ground temperature is given as the surface temperature  $T_{\text{sfc}}$ . For water points, the ground temperature is user specified and held fixed at each point.

To specify the initial conditions on the model grid points, code modifications were made to the appropriate preprocessing routines based on the analytic formulations in steps 1–6.

### 3. Examples

In this section, two examples of initial conditions that were generated using this technique are shown. The examples are 1) zonal flow and 2) continuous sinusoidal waves. The corresponding simulation results are shown for example 1 at 48 h and for example 2 over a 24-h period (24–48 h). In both examples, two domains were used for initialization. The inner (fine) mesh, which was placed over the region of interest (over and downwind from geographic features), had  $61 \times 61 \times 24$  grid points with 30-km resolution. The outer (coarse) mesh, which was used to capture upwind disturbances and to provide improved lateral boundary conditions for the inner (fine) mesh, had  $50 \times 37 \times 24$  grid points with 90-km horizontal resolution. Flat terrain and almost uniform land use were adopted for both examples. The terrain height was set to 1 m at each grid point. Additionally, because development of this technique was motivated by the desire to study the aggregate effects of the Great Lakes

TABLE 1. The parameter values used for initialization of both examples (NA = not applicable).

Parameters	Example 1, zonal flow	Example 2, continuous waves
$h'$ (m)	0.000	$6.000 \times 10^1$
$u_{1000}$ ( $\text{m s}^{-1}$ )	5.000	5.000
dudp [ $\text{m s}^{-1}$ (100 hPa) $^{-1}$ ]	5.000	5.000
$L_{x1000}$ (m)	NA	$3.000 \times 10^6$
$L_{x500}$ (m)	NA	$4.000 \times 10^6$
$x_0$ (m)	NA	$2.740 \times 10^7$
$y_0$ (m)	NA	$4.950 \times 10^3$
$p_0$ (hPa)	NA	$5.000 \times 10^4$
$b_y$ (m)	NA	$7.500 \times 10^5$
$c_{1000}$ ( $\text{m s}^{-1}$ )	NA	$1.800 \times 10^1$
dudp [ $\text{m s}^{-1}$ (100 hPa) $^{-1}$ ]	NA	1.200
tilt (s)	NA	$1.296 \times 10^5$
$C_1$	NA	0.250
$C_2$	NA	0.750

(cf. Sousounis and Fritsch 1994), an idealized pattern of four circular lakes arranged in a square array was placed in the upwind half of the fine mesh domain. This array was intended to represent an idealized configuration for the Great Lakes. The land use was specified to be forest land for each grid point except where there were lakes. The same temperature and humidity profiles for point A, where  $H_A(p)$  was calculated, were used for both examples (Fig. 1). These particular profiles were motivated by conditions that are typically associated with cold air outbreaks for the Great Lakes region in winter. The lake temperatures were specified to be 2°C for the “upper” lakes and 8°C for the “lower” lakes, which are typical lake temperatures for the Great Lakes in November.

The parameter values in the height field formulation for example 1 (zonal flow) are shown in Table 1. The initial sea level pressure (SLP) and 1000–500-hPa thickness fields (output from DATAGRID) for example 1 at 0 h are shown in Fig. 2. Note that because example 1 contained no user-specified disturbances, it was not necessary to prescribe a value for  $c(p)$ . Thus, for the purposes of creating boundary conditions every 12 h, the flow at 12 and 24 h was considered to be the same as that at 0 h. The only variables that needed to be specified to generate height fields were  $h'$ ,  $u_{1000}$  and dudp. Also note that because the zonal wind speed was specified to be a constant on each pressure level, the gradient of the height field was smaller in the south due to the smaller coriolis parameter value.

The initial conditions from example 1 were used to perform a 60-h simulation using MM5. In this simulation, the boundary layer and surface fluxes were turned off in order to test the stability of this initialization technique. The simulated fields from the coarse mesh domain were virtually identical throughout the 60-h simulation to those specified at the initial time. The SLP and 1000–500-hPa thickness fields at 48 h for this simulation are shown in Fig. 3. The steady nature of the simulation results demonstrates that the initial condi-

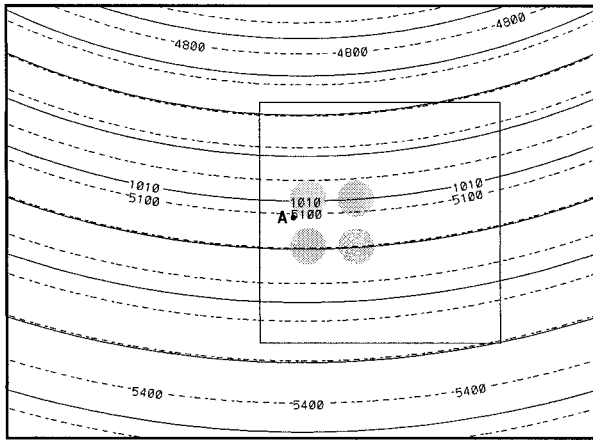


FIG. 2. Coarse grid mesh initialization of sea level pressure (solid, every 2 hPa) and 1000–500-hPa thickness (dashed, every 6 dam) for example 1, zonal flow valid at 0 h. Shaded circles indicate locations of lakes. Inner square indicates 1800 km × 1800 km fine grid mesh (FGM). Point A indicates location of reference thermodynamic profile.

tions were in good physical balance. That is, any imbalances that many have existed initially as a result of interpolation from global to model grids were inconsequential.

The parameter values that were used to specify the initial and boundary conditions for example 2 are shown in Table 1. Note that the values for wavelengths at 1000 and 500 hPa are different and were based on observations of a weak low that developed over the Great Lakes during November 1982 (Sousounis and Fritsch 1994). The phase speeds have been refined according to the measured phase speeds exhibited in the preliminary simulation. The initial SLP and 1000–500-hPa thickness fields for example 2 at 0, 12, and 24 h are shown in

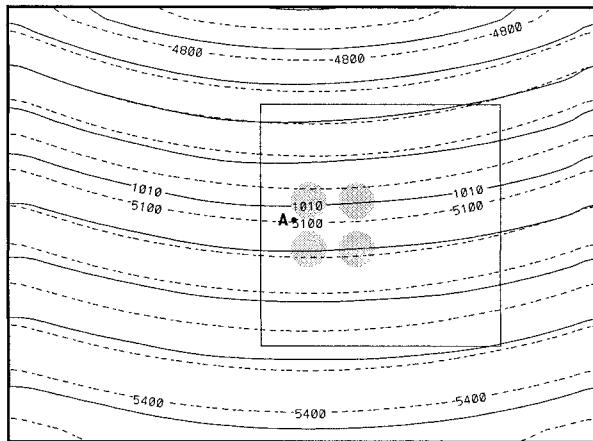


FIG. 3. Coarse grid mesh simulation of sea level pressure (solid, every 2 hPa) and 1000–500-hPa thickness (dashed, every 6 dam) for example 1, zonal flow valid at 48 h. Shaded circles indicate locations of lakes (surface fluxes turned off). Inner square indicates location of FGM. Point A indicates location of reference thermodynamic profile.

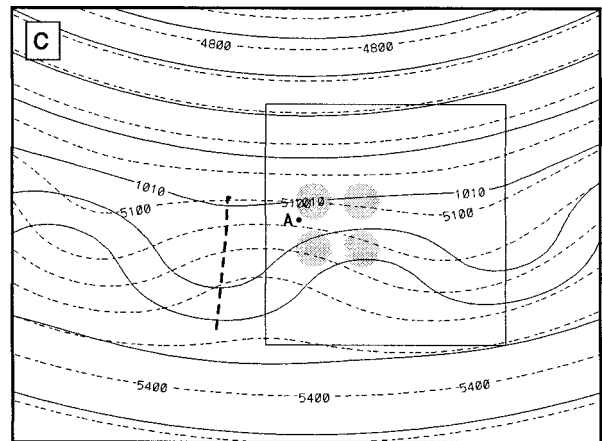
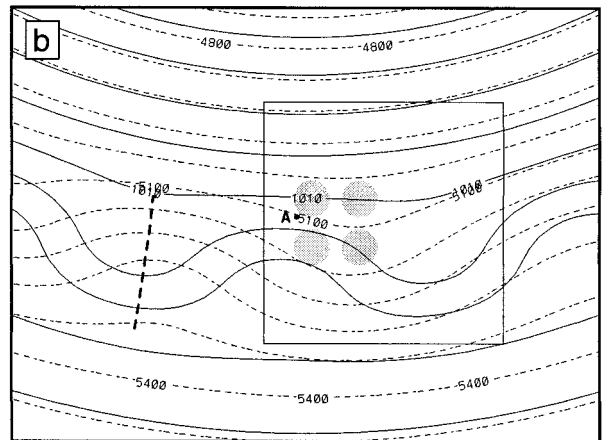
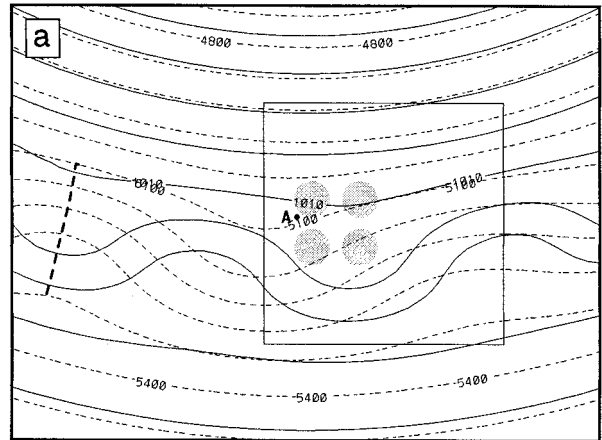


FIG. 4. Coarse grid mesh initialization of sea level pressure (solid, every 2 hPa) and 1000–500-hPa thickness (dashed, every 6 dam) for example 2, continuous sine wave valid at (a) 0, (b) 12, and (c) 24 h. Shaded circles indicate locations of lakes. Inner square indicates location of FGM. Point A indicates location of reference thermodynamic profile. Dashed line indicates location of featured trough.

Fig. 4. Note the distinctly different wavelengths between the two fields. The featured surface low (indicated by the dashed line) was specified to reach optimal vertical tilt with its corresponding 500-hPa trough at 36 h. Be-

cause the geostrophic wind speed was only about 6% larger than the speed of the gradient wind (Holton 1995) in this example, it was feasible to specify the geostrophic wind as the initial wind field. It may be appropriate to substitute gradient wind balance for geostrophic wind balance when specifying initial height fields with more curvature.

For this simulation, the boundary layer and surface fluxes were switched back on and the physical options that were used included the Kuo cumulus scheme, the Blackadar PBL scheme, and the mixed-phase moisture scheme. Description of these schemes can be found in the MM5 documentation by Grell et al. (1994). The simulated SLP and 1000–500-hPa thickness fields from the coarse mesh domain at 24, 36, and 48 h for this example are shown in Fig. 5. Note how a closed low developed by 24 h and how it continued to deepen by  $\sim 11$  hPa over the next 24 h. Realistic asymmetric thermal troughs and ridges (shown) and realistic warm and cold fronts as exhibited by the 1000-hPa temperature fields (not shown) and by the enhanced curvature in the SLP field to the east and south of the (featured) surface low also developed by 48 h. Weak frontogenesis occurred as a normal part of midlatitude cyclone development (Shapiro and Keyser 1990). The weak structure is perhaps a consequence of 1) the fact that the initial conditions (e.g., weak trough) for this case were not intended to generate strong fronts, 2) the relatively short simulation time, and 3) the 30-km resolution.

The impact of the heating and moistening by the (circular) lakes is also evident by the enhanced pressure troughs over the lakes at all three times. While the individual lake-scale troughs are somewhat evident, the larger, lake-aggregate scale effects can really only be identified by comparison of this with-lake simulation to a corresponding no-lake simulation, which is beyond the scope of this study. Notice that there are slight differences in both the SLP and the 1000–500-hPa thickness fields at the CGM boundaries between the initial conditions (Fig. 4c) and the simulation results (Fig. 5a) at 24 h. This is because GRIN, the final preprocessing routine, recalculates the SLP field using slightly different formulations than what was used in DATAGRID.<sup>2</sup> These differences did not affect the simulation—only the graphical output. A further comparison of Fig. 4c and Fig. 5a shows that the surface low propagated only slightly faster than what was user predicted in the initial condition. There was also not much distortion at the boundaries. The lack of distortion adds credibility to the validity of the simulation and demonstrates that the BCs were specified correctly.

#### 4. Closing remarks

This paper describes a technique for specifying idealized initial and boundary conditions. This technique

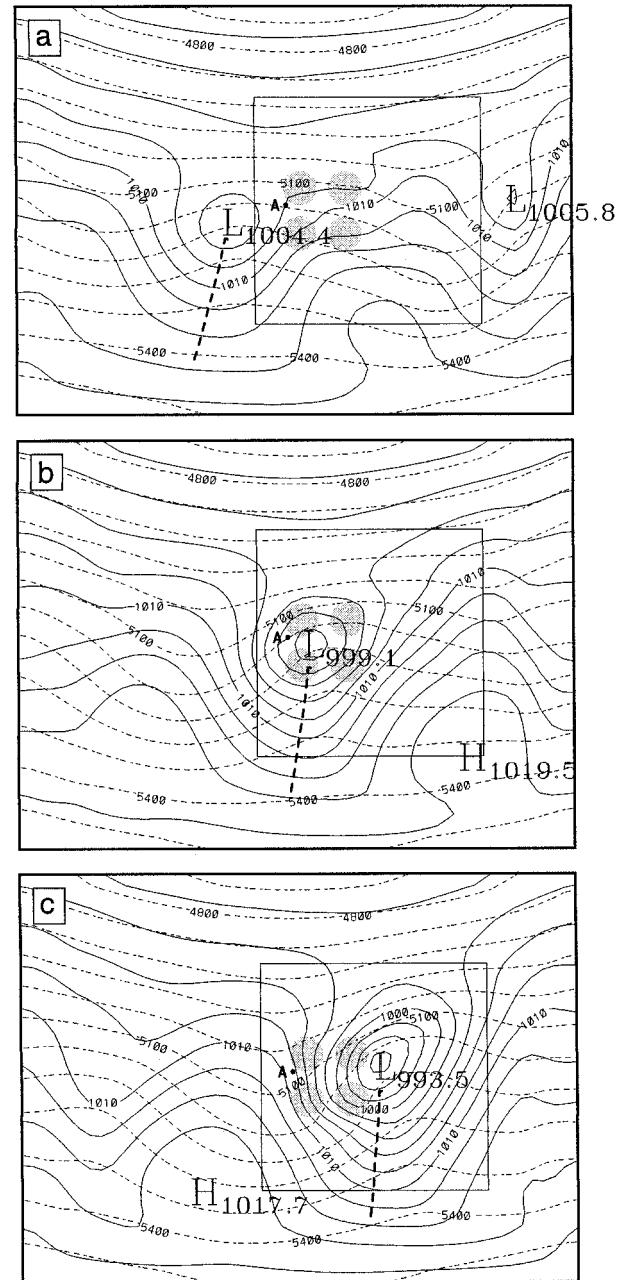


FIG. 5. Coarse grid mesh simulation of sea level pressure (solid, every 2 hPa) and 1000–500-hPa thickness (dashed, every 6 dam) for example 2, continuous sine wave valid at (a) 24, (b) 36, and (c) 48 h. Shaded circles indicate locations of lakes. Inner square indicates location of FGM. Point A indicates location of reference thermodynamic profile. Dashed line indicates location of featured trough.

is capable of simulating a variety of situations, from quiescent flow ( $u_g = 0$  everywhere) to strong synoptic-scale disturbances. In order to demonstrate its utility, the technique was applied to the MM5 modeling system for a specific type of disturbance (example 2). The technique however is easily adaptable to specify different types of disturbances by appropriately modifying

<sup>2</sup> This is true even for the real case initialization of MM5.

[(2.3)]. Although this technique as formulated has not been tested for complex terrain, it may be used to model situations with meso- $\alpha$ -scale or larger terrain features, owing to the fact that good results were obtained with the specified aggregate heat sources at the lower boundary.

Several tasks are planned to improve the flexibility of this technique. They include specifying more complex idealized terrain height and defining disturbances that are capable of moving also in the meridional direction. The latest versions of the idealized initialization routines are available by contacting the corresponding author.

*Acknowledgments.* We would like to thank Dr. David Stauffer for providing us with the MM5 idealized initialization routines for zonal flow. This research was supported by NSF Grant ATM-9502009.

#### REFERENCES

- Ballentine, R. J., A. J. Stamm, E. E. Chermack, G. P. Byrd, and D. Schleede, 1998: Mesoscale model simulation of the 4–5 January 1995 lake-effect snowstorm. *Wea. Forecasting*, **13**, 893–920.
- Cao, Z., and H.-R. Cho, 1995: Generation of moist potential vorticity in extratropical cyclones. *J. Atmos. Sci.*, **52**, 3263–3281.
- Chen, S. S., and W. M. Frank, 1993: A numerical study of the genesis of extratropical convective mesovortices. Part I: Evolution and dynamics. *J. Atmos. Sci.*, **50**, 2401–2426.
- Colle, B. A., and C. F. Mass, 1998: Windstorms along the western side of the Washington Cascade Mountains. Part II: Characteristics of past events and three-dimensional idealized simulations. *Mon. Wea. Rev.*, **126**, 53–71.
- Dudhia, J., 1993: A nonhydrostatic version of the Penn State–NCAR Mesoscale Model: Validation tests and simulation of an Atlantic cyclone and cold front. *Mon. Wea. Rev.*, **121**, 1493–1513.
- Fritch, J. M., E. L. Magaziner, and C. F. Chappell, 1980: Analytical initialization for three-dimensional models. *J. Appl. Meteor.*, **19**, 809–818.
- Grell, G. A., J. Dudhia, and D. R. Stauffer, 1994: A description of the fifth-generation Penn State/NCAR Mesoscale Model (MM5). NCAR Tech. Note NCAR/TN-398+STR, 23 pp.
- Haltiner, G. J., and R. T. Williams, 1980: *Numerical Prediction and Dynamic Meteorology*. 2d ed. John Wiley and Sons, 477 pp.
- Holton, J. R., 1995: *An Introduction to Dynamic Meteorology*. 3d ed. Academic Press, 511 pp.
- Nuss, W. A., and R. A. Anthes, 1987: A numerical investigation of low-level processes in rapid cyclogenesis. *Mon. Wea. Rev.*, **115**, 2728–2743.
- Shapiro, M. A., and D. Keyser, 1990: Fronts, jet streams and the tropopause. *Extratropical Cyclones: The Erik Palmén Memorial Volume*, C. Newton and E. O. Holopainen, Eds., Amer. Meteor. Soc., 167–191.
- Sousounis, P. J., and J. M. Fritsch, 1994: Lake aggregate mesoscale disturbances. Part II: A case study of the effects on regional and synoptic scale weather systems. *Bull. Amer. Meteor. Soc.*, **75**, 1793–1812.
- Stauffer, D. R., N. L. Seaman, T. T. Warner, and A. M. Lario, 1993: Application of an atmospheric simulation model to diagnose air pollution transport in the Grand Canyon region of Arizona. *Chem. Eng. Commun.*, **121**, 9–26.
- Sun, W. Y., and J.-D. Chern, 1994: Numerical experiments of vortices in the wakes of large idealized mountains. *J. Atmos. Sci.*, **51**, 191–209.